I&EC research
Industrial & Engineering Chemistry Research

ARTICLE

pubs.acs.org/IECR

Preparation of Oriented Layered Double Hydroxide Film Using Electrophoretic Deposition and Its Application in Water Treatment

Shan He, Yufei Zhao, Min Wei,* and Xue Duan

State Key Laboratory of Chemical Resource Engineering, Beijing University of Chemical Technology, Beijing 100029, People's Republic of China

S *Supporting Information*

ABSTRACT: Oriented Mg/Al$-$NO$_3$-layered double hydroxide (LDH) films have been fabricated by the electrophoretic deposition method (EPD) on aluminum substrate, which can be used to remove heavy metal ion and anionic dye from aqueous solutions. The LDH films with thickness of ~4 μm by EPD method show a high degree of *c*-orientation of the LDH platelets (the *ab*-plane parallel to the substrate) and strong adhesion to the substrate confirmed by XRD and SEM. The sorption kinetics of the LDH film for Cr(VI) and Remazol Brilliant Blue R dye (RBBR) was appropriately described by the pseudo-second-order model. Sorption isotherms for Cr(VI) and RBBR by the LDH film were studied, which can be fitted by the Langmuir model more satisfactorily than by the Freundlich model. It was found that the sorption capacity (q_{MAX}) reached ~79.4 mg g^{-1} for Cr(VI) and ~222 mg g^{-1} for RBBR respectively, much larger than that of the corresponding LDH powder sample (~67.6 mg g^{-1} for Cr(VI) and ~192.3 mg g^{-1} for RBBR, respectively). Furthermore, the LDH film exhibits excellent sorption$-$regeneration performances as compared to the powder sample, which facilitates its repeatable and cyclic usage over a long period. Because of the low-cost preparation, high sorption capacity, convenient manipulation, as well as easy regeneration of the LDH film, it is expected that this film can be potentially used as a structured adsorbent in the field of water treatment.

1. INTRODUCTION

In recent years, layered double hydroxides (LDHs) as a class of anionic clays have attracted considerable attention from both industry and academia because of their potential applications in areas such as catalysis,[1] sorption,[2,3] functional materials,[4] and drug delivery.[5] LDHs can be represented by the general formula $[\mathrm{M}^{2+}{}_{1-x}\mathrm{M}^{3+}{}_{x}(\mathrm{OH})_2]^{x+}(\mathrm{A}^{n-}{}_{x/n})\cdot m\mathrm{H_2O}$, where M^{2+} and M^{3+} are divalent and trivalent metal cations, respectively, and A^{n-} is an anion. The host structure consists of brucite-like layers of edge-sharing $\mathrm{M(OH)_6}$ octahedra, and the partial substitution of M^{3+} for M^{2+} induces positively charged host layers, balanced by the interlayer anions.[6] A large number of isostructural LDH materials with specific physicochemical properties can be obtained by changing the identity of metal cations, the molar ratio of $\mathrm{M}^{2+}/\mathrm{M}^{3+}$, as well as the interlayer anions.

Heavy metal ions and synthetic dyes entering the environment as toxic wastes give rise to potentially serious environmental problems throughout the world. Cr(VI), widely existing in the effluents of electroplating, tanning, mining, and fertilizer industries, is a carcinogenic contaminant to humans.[7] Remazol Brilliant Blue R (RBBR, an anthraquinone derivative), widely applied as organic dye in the textile industry, is a carcinogenic and mutagenic pollutant for humans and aquatic organisms.[8] As LDH materials exhibit large specific surface area,[9] high anion exchange capacity,[10] and calcination$-$reconstruction property,[11] they have been widely used as powder adsorbents to remove heavy metal ions[12−15] and other contaminants[16−18] from wastewater. It was reported that the removal of contaminants by LDHs from solution relates to three mechanisms: (1) surface sorption,[19] (2) intercalation by anion exchange,[20] and (3) intercalation by reconstruction of the calcined LDH structure.[21] However, the application of LDH powder sorbents shows the following drawbacks: the formation of aggregates, and the difficulties in subsequent separation, regeneration, and recycling process. From this point of view, the application of immobilized LDH film as structured adsorbents is one effective solution to these problems, for they may possess the advantages of high dispersion of LDH microcrystals, easy regeneration, and manipulation. Various methods have been reported for the fabrication of LDH films. Liu et al.[22] used delaminated CoAl$-$LDH nanosheets to prepare multilayer ultrathin films through the layer-by-layer self-assembly technique; Lee and co-worker[23] employed the ultrasonification method to prepare a monolayer of LDH films. Recently, our group[24] reported the preparation of Ni/Al$-$LDH films on a PAO/Al substrate via in situ crystallization technique.

The electrophoretic deposition method (EPD) is one effective technique to fabricate films and devices, which possesses advantages of simplicity in equipment setup, high deposition rate, easy control of the thickness/morphology, and strong adhesion to substrates.[25] In the EPD process, charged particles, dispersed or suspended in a liquid medium, are attracted and deposited onto a conductive substrate of opposite charge on application of a DC electric field.[26] This method has been successfully used for the preparation of nanosize zeolite membrane,[27] high-T_c superconducting

Received: May 25, 2010
Accepted: December 22, 2010
Revised: December 22, 2010
Published: January 24, 2011

films,[28] gas diffusion electrodes and sensors,[29] as well as carbon nanotube film.[30]

In the present work, we report the fabrication of oriented LDH films by the EPD technique on aluminum substrate and demonstrate its application in water treatment. The MgAl−LDH films obtained show a well *c*-orientation of LDH platelets and strong adhesion to the substrate. Cr(VI) and Remazol Brilliant Blue R dye (RBBR) were chosen as highly toxic pollutants in water, and their sorption by the LDH films was studied thoroughly. The pseudo-second-order model can be used to describe the sorption kinetics of Cr(VI) and RBBR. The Langmuir model yields a much better fit than does the Freundlich model to describe the two sorptions satisfactorily. It was found that both the sorption capacity and the kinetics are much higher than that of the LDH powder as a comparison sample; moreover, the LDH film exhibits more stable sorption−regeneration behavior and convenient manipulation as compared to the powder sample. Therefore, this work provides a facile and effective method for the fabrication of oriented LDH film, which can be used as a structured adsorbent in water treatment with low cost, high capability, recycle, and long-life usage.

2. EXPERIMENTAL METHOD

2.1. Materials. RBBR (CI 61200, Reactive Blue 19) was purchased from Sigma-Aldrich Co. Analytical grade chemicals including $Mg(NO_3)_2 \cdot 6H_2O$, $Al(NO_3)_3 \cdot 9H_2O$, NaOH, $K_2Cr_2O_7$, and anhydrous ethanol were purchased from the Beijing Chemical Co. Ltd. and used without further purification. Aluminum metal sheet was purchased from Shanghai Jing Xi Chemical Technology Co. Ltd., purity > 99.5%, thickness of 0.2 mm. The deionized and decarbonated water was used in all the experimental processes.

2.2. Preparation of the Mg_2Al-NO_3-LDH Colloidal Suspension. The Mg_2Al-NO_3-LDH colloidal suspension was prepared by the hydrothermal method reported previously.[31] A solution of $Mg(NO_3)_2 \cdot 6H_2O$ (0.06 mol) and $Al(NO_3)_3 \cdot 9H_2O$ (0.03 mol) in 75 mL of water was quickly added to 75 mL of NaOH solution (2.4 M) with vigorous agitation under nitrogen atmosphere. The mixture was transferred into an autoclave, followed by hydrothermal treatment at 110 °C for 24 h. The precipitate was separated by centrifugation and washed thoroughly with water. Afterward, the colloidal nanoparticle suspension of Mg_2Al-NO_3-LDH (about 20 g L^{-1}) for EPD is obtained by fresh precipitate ultrasonically dispersed in ethanol.

2.3. Fabrication of the Oriented LDH Film by the EPD Method. Al metal sheet was polished by sand paper to remove the oxide layer and ultrasonically treated in ethanol and deionized water, respectively, prior to deposition of the LDH film. The film of Mg_2Al-NO_3-LDH was fabricated by the EPD method (the schematic illustration of the setup is shown in Figure S1).[26] The constant DC potential was applied between the working (Al substrate) and counter electrode (stainless steel plate). The parallel distance between two electrodes is 15 mm, and the applied voltage and deposition time are 20 V and 5 min, respectively. The LDH film immobilized on the surface of working electrode was washed by water and dried in air at room temperature for 12 h.

2.4. The Evaluation of LDH Film as Adsorbent. *2.4.1. The Sorption of Cr(VI).* The LDH film with 170 mg of sorbent was immersed into 200 mL of $K_2Cr_2O_7$ solution (20 mg L^{-1}) at ambient temperature with constant shaking. The pH of $K_2Cr_2O_7$ solution was adjusted to 6.0 and maintained during the process of sorption. A 1 mL aliquot was filtered from the solutions at specific time intervals using a 0.45 μm membrane filter. The concentration of Cr(VI) in the filtrate was analyzed using ICP-ES.

2.4.2. The Sorption of RBBR. Sorption experiments of RBBR were carried out in 300 mL stoppered conical flask at room temperature. The LDH film with 125 mg of sorbent was immersed into 250 mL of RBBR solution (50 mg L^{-1}) with constant shaking. The pH of RBBR solution was ∼7.5 without control during the process of sorption. At specified time intervals, 1 mL of solution was removed and filtered through a 0.45 μm membrane filter. The concentration of RBBR in the filtrate was determined by UV−vis spectroscopy. The absorbance was measured at 593 nm.

2.4.3. The Sorption Capacity (q_e) and the Removal Percentage (R%).

$$q_e = \frac{(c_0 - c_e)V}{m} \tag{1}$$

$$R\% = 100 \times \frac{c_0 - c_e}{c_0} \tag{2}$$

where c_0 is the initial concentration of Cr(VI) or RBBR in solution (mg L^{-1}); c_e is the equilibrium concentration (mg L^{-1}); q_e is the equilibrium sorption capacity (mg g^{-1}); m is the mass of adsorbent (g); and V is the volume of solution (L).

2.4.4. Sorption Isotherms. The sorption isotherms for Cr(VI) and RBBR were established by batch type sorption experiments. The LDH films with 35 and 30 mg of sorbent, respectively, were immersed into 40 mL of Cr(VI) solution (from 5 to 120 mg L^{-1}) and a60 mL of RBBR solution (from 25 to 600 mg L^{-1}) at ambient temperature with constant shaking, until the sorption equilibrium was obtained. The pH of Cr(VI) solution was controlled at 6.0, while the RBBR solution remained at 7.5 without disturbance during the process of sorption.

2.4.5. Test for the Sorption−Regeneration Recycles. Desorption/regeneration measurements were performed by immersing the Cr(VI)-loaded LDH film into 100 mL of Na_2CO_3 solution (0.01 mol L^{-1}) with constant shaking at 30 °C.[2] At selected time intervals, 1 mL of sample was extracted, and the concentration of Cr(VI) was determined by ICP-ES. Sorption−regeneration tests were consecutively repeated five times by the same methods described above to study the sorption properties of the regenerated LDH film.

2.5. Characterization Technique. The powder X-ray diffraction (XRD) measurements were performed on a Rigaku XRD-6000 diffractometer, using Cu−Kα radiation (λ = 0.15418 nm) at 40 kV, 30 mA, with a scanning rate of 10° min^{-1}, and a 2θ angle ranging from 3° to 70°. The morphology of the LDH film was investigated by using a Hitachi S-4700 scanning electron microscope (SEM) fitted with an Oxford Instruments Isis-300 energy dispersive X-ray (EDX) analyzer operating at 20 kV. A UV−vis spectrophotometer (Beijing PGENERAL TU-1901) was employed to measure the absorption spectra of RBBR in the wavelength range 200−700 nm. Inductively coupled plasma emission spectroscopy (ICP-ES, Shimadzu ICPS-7500) was used to measure the concentration of Cr(VI) in the solution.

3. RESULTS AND DISCUSSION

3.1. Structure and Orientation of LDH Films by the EPD Method. Figure 1 illustrates the XRD pattern of the Mg/Al−LDH film (Figure 1b) on the Al substrate by the EPD method, with the pristine Al substrate (Figure 1a) and Mg/Al−LDH powder sample (Figure 1c) for the purposes of comparison. For the LDH film (Figure 1b) and powder sample (Figure 1c), XRD patterns exhibit the characteristic reflections of the LDH structure with a series of (00*l*) reflections appearing as narrow, symmetric, strong lines at low angles. The basal spacing for the film and powder sample is 0.863 and 0.885 nm, respectively, close to the value reported for NO_3^--containing LDHs.[32] In the case of the LDH film sample, the absence of any nonbasal reflections ($h, k \neq 0$) at high angle is as expected for extremely well *c*-oriented assemblies of LDH microcrystals, which indicates that the *ab*-plane of the LDH platelets is parallel to the substrate.[33] In contrast, the LDH powder sample displays additional (012), (110), and (113) reflections, indicative of diffuse scattering arising from irregular stacking of LDH microcrystals.

SEM images of the LDH film are shown in Figure 2. The film exhibits a surprisingly smooth and flat surface without any cracking in the top view (Figure 2a). A high-magnification SEM image of the film (Figure 2b) reveals that the individual LDH platelets (particle size of 100−160 nm) are densely packed in the two-dimensional plane of the film with a high degree of *c*-orientation (*ab*-plane of the microcrystal parallel to the substrate). The film thickness of ~4 μm can be observed from the side view of SEM image (Figure 2c), and the high-magnification image (Figure 2d) shows the anisotropy of the film with face-to-face stacking between individual LDH platelets. This is in accordance with the result of XRD. It also can be seen from Figure 2d that the film possess a loose and microporous architecture in the vertical direction. Furthermore, no delamination or peeling occurred on cross-cutting the film surface, indicating strong adhesion of the film to the substrate (Figure 2e).[34] However, the LDH powder sample shows irregular and random packing with the formation of aggregates, as shown in Figure 2f. It can be concluded that the fabrication of *c*-oriented LDH film with strong mechanical stability was achieved by the EPD method. The specific structure of LDH film would be beneficial to the diffusion and sorption of Cr(VI) and RBBR, which will be further discussed below.

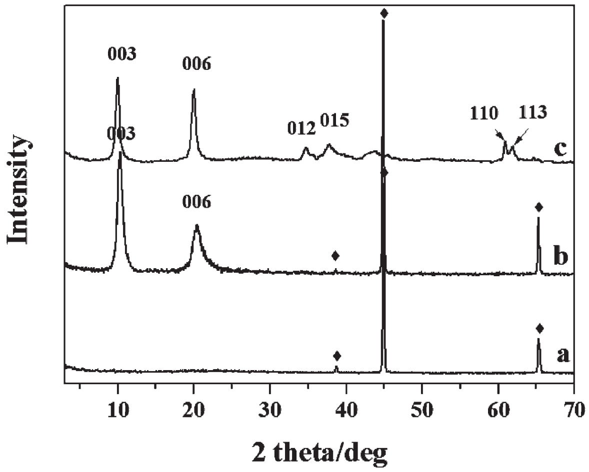

Figure 1. XRD patterns of (a) Al substrate, (b) Mg/Al−LDH film, and (c) Mg/Al−LDH powder sample. The rhombic symbol indicates the reflections from the Al substrate.

3.2. The Sorption Behavior of Cr(VI) and RBBR on the LDH Film. The LDH film obtained by the EPD method was used to remove Cr(VI) and anionic dye (RBBR) from aqueous solution, and the sorption performance of the LDH film was investigated for Cr(VI) and Remazol Brilliant Blue R dye (RBBR) in this work. Figure 3A shows the effect of contact time on the sorption capacity of Cr(VI) by the LDH film and the corresponding powder sample. It was found that the self-sorption of Cr(VI) on Al substrate was hardly observed, while the MgAl−LDH powder sample shows sorption ability for Cr(VI), with the removal percentage of ~70% after 250 min. As compared to the powder sample, the MgAl−LDH film exhibits higher sorption capability. A removal percentage of ~94% [(Cr(VI)] was achieved after 250 min. Moreover, the sorption capacity of the film sample for Cr(VI) reaches 8.2 mg g^{-1}, much larger than that of the powder sample (6.1 mg g^{-1}). In addition, the sorption behavior of the LDH film for RBBR was also studied (Figure 3B). In the case of the LDH powder sample, the sorption capacity at equilibrium for RBBR was 62 mg g^{-1} and removal percentage was 62%. In contrast, the sorption capacity and removal percentage by the

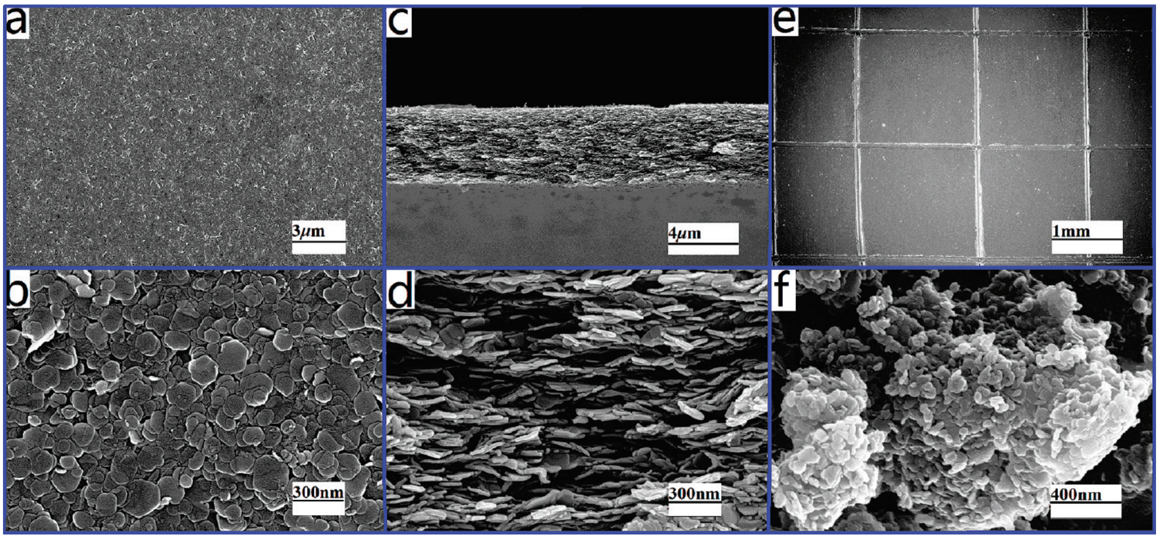

Figure 2. SEM images of the MgAl−LDH film by the EPD method on Al substrate: top view with (a) low- and (b) high-magnification; side view with (c) low- and (d) high-magnification; (e) the LDH film tested for adhesion; and (f) the LDH powder sample.

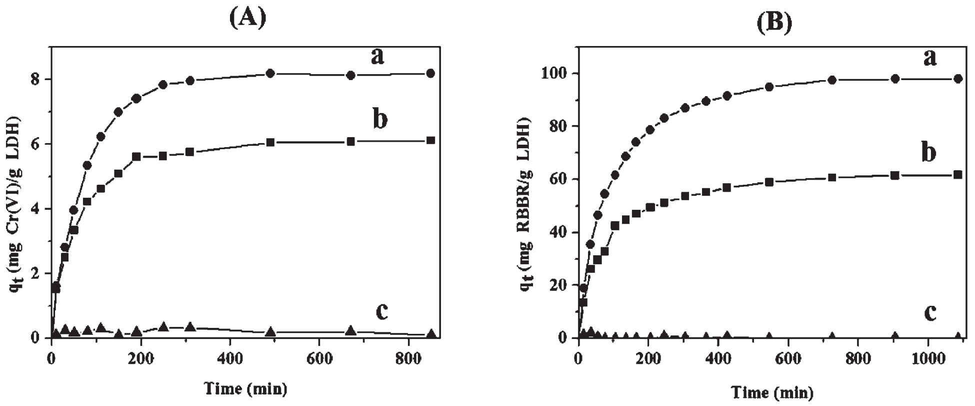

Figure 3. (A) The effect of contact time on the sorption capacity for chromium(VI) ([$K_2Cr_2O_7$], 20 mg L^{-1}; volume, 200 mL; dosage of adsorbent, 170 mg; 20 °C; pH = 6); (B) the effect of contact time on the sorption capacity for RBBR ([RBBR], 50 mg L^{-1}; volume, 250 mL; dosage of adsorbent, 125 mg; 20 °C): (a) the LDH film, (b) the LDH powder sample, and (c) the Al substrate.

Table 1. Kinetic Parameters for the Sorption of Cr(VI) and RBBR by the LDH Film Based on the Pseudo-Second-Order Model

adsorbate	$q_{e,exp}$ (mg g^{-1})	k_2 (g mg^{-1} min^{-1})	$q_{e,cal}$ (mg g^{-1})	R^2
Cr(VI)	8.2	2.55×10^{-3}	8.7	0.9981
RBBR	98.1	1.40×10^{-4}	105.3	0.9997

LDH film reached 98 mg g^{-1} and 95%, respectively. It is obvious that the LDH film by the EPD method exhibits a better sorption performance for Cr(VI) and RBBR compared with LDH powder. The poor sorption capability of the LDH powder sample is probably due to the formation of aggregates (Figure 2f), which is generally inevitable for nanoscale materials. In contrast, well *c*-oriented assemblies of LDH microcrystals on Al substrate without aggregation as well as the loose and microporous film structure (Figure 2d) provide large specific surface area, resulting in better sorption performance of the LDH film, but the conventional nitrogen adsorption and desorption measurements for the specific surface area and micropore volume of the LDH film are very difficult for its rather thin thickness (~4 μm). Moreover, it was found that a transformation from NO_3^-—LDH ($2\theta = 10.2°$) to CO_3^{2-}—LDH ($2\theta = 11.5°$) occurred after the sorption process (Figure S2), which indicates that the sorption process mainly occurs on the surface of the LDH film. This is related to the low concentration of pollutants studied in this work (20 mg L^{-1} for $K_2Cr_2O_7$ and 50 mg L^{-1} for RBBR), resulting in a weak sorption driving force based on the concentration gradient.

Sorption kinetics was studied to explain the sorption mechanism and characteristics of Cr(VI) or RBBR on the LDH film. Ho's pseudo-second-order model[35,36] was chosen for the description of the sorption process for Cr(VI) and RBBR:

$$\frac{t}{q_t} = \frac{1}{k_2 q_e^2} + \frac{t}{q_e} \tag{3}$$

where q_e and q_t (mg g^{-1}) are the amounts of Cr(VI) or RBBR adsorbed on the LDH film at equilibrium and at time t (min), respectively; k_2 (g mg^{-1} min^{-1}) is the rate constant of the pseudo-second-order kinetic model. The linear relationship of t/q_t versus t is presented in Figure S3. The values of q_e and k_2 can be calculated from the slope and intercept of the plot, respectively, which are listed in Table 1. It can be seen that the pseudo-second-order kinetic model can be satisfactorily used to describe the sorption behavior of Cr(VI) and RBBR on the LDH film in terms of high correlation coefficients ($R^2 > 0.99$). In addition, the calculated sorption capacity ($q_{e,cal}$) obtained from the model is quite close to the experimental one ($q_{e,exp}$). As a result, the sorption kinetics fitted well with the pseudo-second-order model, which suggests that the sorption process of Cr(VI) and RBBR on the LDH film involves a chemisorption process that is the rate-limiting step.[35,36]

3.3. The Sorption Isotherms for Cr(VI) and RBBR. Sorption isotherms were investigated to exhibit the sorption capacity of the LDH film for Cr(VI) and RBBR, respectively (Figure 4). Two commonly used sorption isotherm models were used to fit the equilibrium data: Langmuir (eq 4) and Freundlich (eq 5).[37]

$$\frac{C_e}{q_e} = \frac{1}{K_L q_{MAX}} + \frac{C_e}{q_{MAX}} \tag{4}$$

$$\ln q_e = \ln K_F + \frac{1}{n} \ln c_e \tag{5}$$

where q_e (mg g^{-1}) is the amount of Cr(VI) or RBBR adsorbed on the LDH film at equilibrium; C_e (mg L^{-1}) is the concentration at equilibrium; q_{MAX} (mg g^{-1}) is the theoretical maximum monolayer sorption capacity; K_L (L mg^{-1}) is the Langmuir sorption constant; K_F (L g^{-1}) is the Freundlich constant; and $1/n$ is the heterogeneity factor. It can be seen that the Langmuir model yields a much better fit than does the Freundlich model based on the value of R^2 listed in Table 2. In addition, the sorption capacity (q_{MAX}) reaches ~79.4 mg g^{-1} for Cr(VI) and ~222 mg g^{-1} for RBBR, respectively, much larger than that of the corresponding LDH powder sample (~67.6 mg g^{-1} for Cr(VI) and ~192.3 mg g^{-1} for RBBR, respectively).

3.4. Sorption—Regeneration of the LDH Film for Recycle Application. Because the sorption—regeneration of adsorbents is the most difficult and expensive part of an sorption technology, a successful sorption—regeneration process is very important to gain an efficient and low-cost technique for wastewater treatment systems.[38] The regeneration and recycle application of the LDH film adsorbent was demonstrated through the Cr(VI)-containing solution. Desorption of Cr(VI) from the LDH film was carried out in a Na_2CO_3 solution to evaluate the regeneration behavior of the adsorbent, and Figure 5 shows the desorption percentage of Cr(VI) as a function of time from the LDH film and powder adsorbent, respectively. It was found that a close desorption

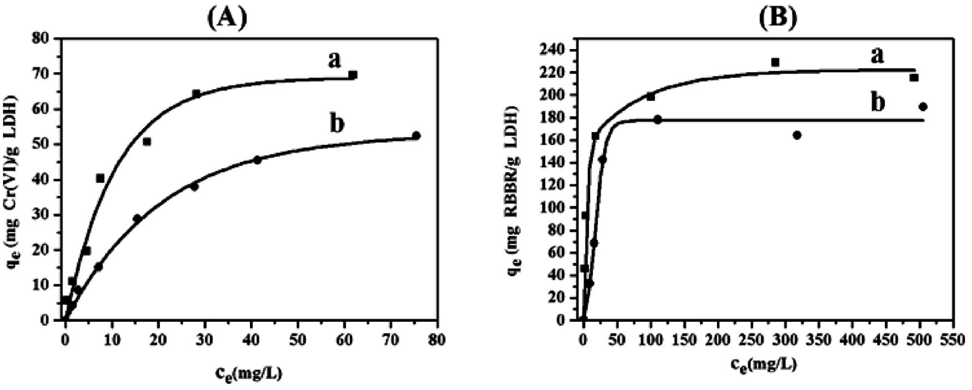

Figure 4. Sorption isotherms for (A) Cr(VI) and (B) RBBR: (a) the LDH film, and (b) the LDH powder sample.

Table 2. Langmuir and Freundlich Isotherm Parameters for the Sorption of Cr(VI) and RBBR

	Langmuir			Freundlich		
adsorbent	q_m (mg g^{-1})	K_L (L mg^{-1})	R^2	n	K_F (L g^{-1})	R^2
sorption of Cr(VI) by the LDH film	79.4	0.118	0.9765	2.026	11.043	0.9567
sorption of Cr(VI) by the LDH powder	67.6	0.046	0.9956	1.552	4.058	0.9728
sorption of RBBR by the LDH film	222.2	0.175	0.9983	4.014	56.764	0.8257
sorption of RBBR by the LDH powder	192.3	0.037	0.9905	2.790	24.695	0.7120

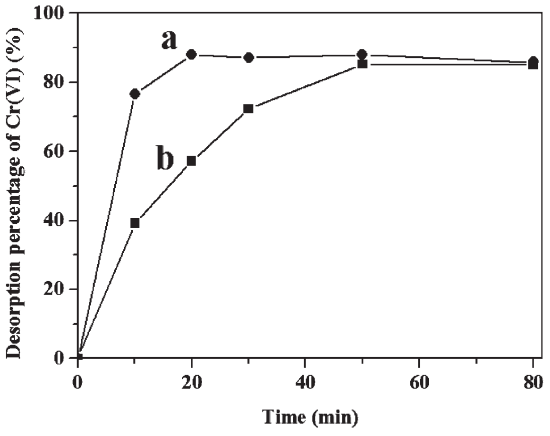

Figure 5. Desorption percentage of Cr(VI) from (a) the LDH film and (b) the LDH powder sample as a function of time (100 mL of 0.01 M Na_2CO_3 solution at 30 °C).

capacity can be obtained for the two adsorbents (88% for film and 85% for powder), while the LDH film shows a much faster desorption process than does that of the powder sample (20 vs 50 min for equilibrium).

The consecutive sorption−regeneration cycles for Cr(VI) by the LDH film and powder sample, respectively, were repeated five times under uniform experimental conditions, and the sorption capacity for each cycle is shown in Figure 6. The sorption capacity of the LDH powder sample for the first cycle is 6.1 mg g^{-1}, but it decreases to 2.5 mg g^{-1} for the subsequent cycles. As compared to the LDH powder sample, the film adsorbent not only shows larger initial sorption capacity (8.2 mg g^{-1}) but also maintains higher value (~5.0 mg g^{-1}) in the consecutive cycles of sorption−regeneration. The superior sorption−regeneration properties of the LDH film adsorbent are attributed to its oriented packing and microporous structure; moreover, no obvious change in its morphology can be found after five cycles (Figure 7a and b). Additionally, no leaching of adsorbent from the substrate can be detected, due to the strong mechanical stability of the LDH film as mention above. For the powder sample, however, serious aggregation of LDH nanoparticles occurs after five cycles (shown in Figure 7c and d), which imposes great influence on the sorption−desorption process and results in low sorption capacity.

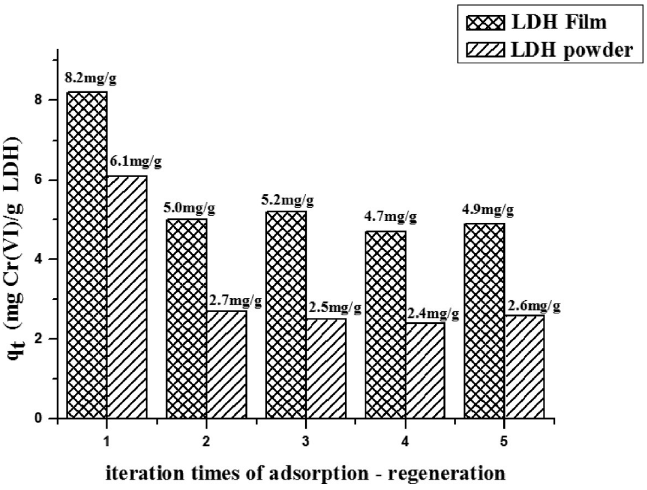

Figure 6. The sorption capacity of Cr(VI) by the LDH film and powder adsorbent respectively for five consecutive cycles of sorption−regeneration.

To give a further understand of the decrease in sorption capacity after the first cycle, the XRD patterns of the as-prepared LDH film and after the first as well as the fifth cycles were measured and shown in Figure 8. It was found that the basal spacing (d_{003}) of the LDH film after the first sorption−regeneration

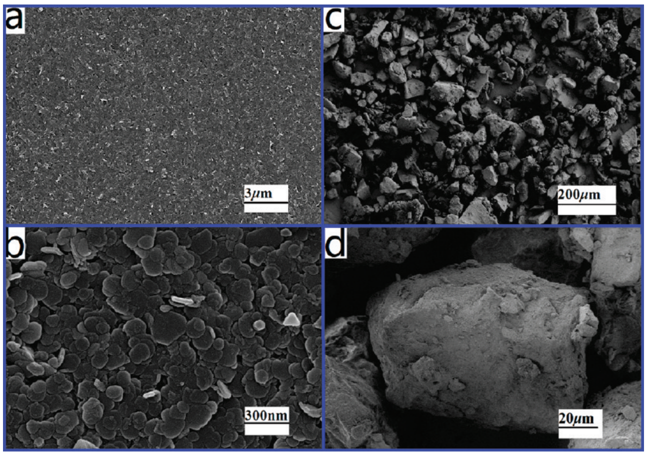

Figure 7. SEM images of the LDH film after five consecutive cycles of sorption−regeneration: (a) low-magnification, (b) high-magnification. SEM images of the powder sample after five cycles: (c) low-magnification, (d) high-magnification.

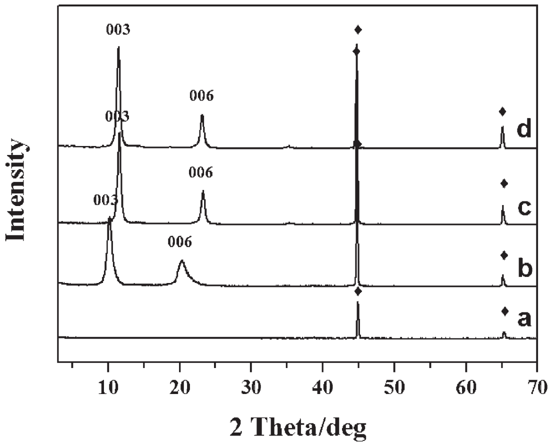

Figure 8. XRD patterns of (a) Al substrate, (b) the Mg/Al−LDH film as prepared, (c) the Mg/Al−LDH film after first cycle of sorption−regeneration, and (d) the Mg/Al−LDH film after five consecutive cycles. The rhombic symbol indicates the reflections from the Al substrate.

cycle decreases from 0.863 nm (Figure 8b, the freshly prepared NO_3^-−LDH) to 0.765 nm (Figure 8c), which is in agreement with the value reported for LDH with CO_3^{2-} anion.[39] This interlayer distance remains unchanged during the following cycles (Figure 8d). This indicates that carbonate was intercalated into LDH gallery during the process of regeneration. Therefore, the decrease in sorption capacity in the subsequent cycles is probably due to particularly high affinity between carbonate and the interlayer region of LDH.

4. CONCLUSIONS

We have demonstrated a facile approach for the fabrication of LDH film on Al substrate with a high degree of *c*-orientation of the LDH platelets and strong adhesion to the substrate. The film prepared by EPD shows superior sorption capability for Cr(VI) and RBBR as compared to the corresponding LDH powder sample, due to the high dispersion of LDH microcrystals on Al substrate without aggregation as well as the loose and microporous film structure. The sorption kinetics of Cr(VI) and RBBR on LDH film is satisfactorily described by the pseudo-second-order model. The Langmuir model yields a much better fit than does the Freundlich model to describe the two sorptions satisfactorily. In addition, the LDH film exhibits excellent sorption−regeneration performances, facilitating its repeatable and cyclic usage over a long period. Therefore, the LDH film in this work exhibits the advantages of large sorption capability, strong mechanical robustness, convenient manipulation, as well as easy regeneration and recycling for water treatment. It is expected that this oriented and high-quality LDH film by the EPD can be potentially used as efficient and recycling adsorbents in water treatment. The sorption behavior of the LDH film in real wastewater as an in-depth research is underway in our lab.

■ ASSOCIATED CONTENT

Ⓢ Supporting Information. Additional figures. This material is available free of charge via the Internet at http://pubs.acs.org.

■ AUTHOR INFORMATION

Corresponding Author

*Tel.: +86-10-64412131. Fax: +86-10-64425385. E-mail: weimin@mail.buct.edu.cn.

■ ACKNOWLEDGMENT

This project was supported by the National Natural Science Foundation of China, the 111 Project (Grant No. B07004), and the 973 Program (Grant No. 2011CBA00504).

■ REFERENCES

(1) Liu, H. C.; Min, E. Z. Catalytic Oxidation of Mercaptans by Bifunctional Catalysts Composed of Cobalt Phthalocyanine Supported on Mg−Al Hydrotalcite-derived Solid Bases:Effects of Basicity. *Green Chem.* **2006**, *8*, 657–662.

(2) Lazaridis, N. K.; Pandi, T. A.; Matis, K. A. Chromium(VI) Removal from Aqueous Solutions by Mg-Al-CO_3 Hydrotalcite: Sorption-desorption Kinetic and Equilibrium Studies. *Ind. Eng. Chem. Res.* **2004**, *43*, 2209–2215.

(3) Dadwhal, M.; Ostwal, M. M.; Liu, P. K. T.; Sahimi, M.; Tsotsis, T. T. Adsorption of Arsenic on Conditioned Layered Double Hydroxides: Column Experiments and Modeling. *Ind. Eng. Chem. Res.* **2009**, *48*, 2076–2084.

(4) Yan, D. P.; Lu, J.; Wei, M.; Han, J. B.; Ma, J.; Li, F.; Evans, D. G.; Duan, X. Ordered Poly(p-phenylene)/Layered Double Hydroxide Ultrathin Films with Blue Luminescence by Layer-by-Layer Assembly. *Angew. Chem., Int. Ed.* **2009**, *121*, 3119–3122.

(5) Khan, A. I.; Lei, L.; Norquist, A. J.; O'Hare, D. Intercalation and Controlled Release of Pharmaceutically Active Compounds from a Layered Double Hydroxide. *Chem. Commun.* **2001**, *22*, 2342–2343.

(6) Evans, D. G.; Slade, R. C. T. Structural Aspects of Layered Double Hydroxides. *Struct. Bonding (Berlin)* **2005**, *119*, 1–87.

(7) Cieslak-Golonka, M. Toxic and Mutagenic Effects of Chromium (VI). *Polyhedron* **1995**, *15*, 3667–3689.

(8) Eichlerová, I.; Homolka, L.; Benada, O.; Kofroňová, O.; Hubálek, T.; Nerud, F. Decolorization of Orange G and Remazol Brilliant Blue R by the White Rot Fungus Dichomitus Squalens: Toxicological Evaluation and Morphological Study. *Chemosphere* **2007**, *69*, 795–802.

(9) Cavani, F.; Trifir, F.; Vaccari, A. Hydrotalcite-type Anionic Clays: Preparation, Properties and Applications. *Catal. Today* **1991**, *11*, 173–301.

(10) Meyn, M.; Beneke, K.; Lagaly, G. Anion-Exchange Reactions of Layered Double Hydroxides. *Inorg. Chem.* **1990**, *29*, 5201–5207.

(11) Châtelet, L.; Bottero, J. Y.; Yvon, J.; Bouchelaghem, A. Competition between Monovalent Anions for Calcined and Uncalcined Hydrotalcite: Anion Exchange and Adsorption Sites. *Colloids Surf,. A* **1996**, *111*, 167–75.

(12) Türk, T.; Alp, İ.; Deveci, H. Adsorption of As(V) from Water Using Mg—Fe-based Hydrotalcite (FeHT). *J. Hazard. Mater.* **2009**, *171*, 665–670.

(13) Wang, S. L.; Hseu, R. J.; Chang, R. R.; Chiang, P. N.; Chen, J. H.; Tzou, Y. M. Adsorption and Thermal Desorption of Cr(VI) on Li/Al Layered Double Hydroxide. *Colloids Surf., A* **2006**, *277*, 8–14.

(14) Yang, L.; Shahrivari, Z.; Liu, P. K. T.; Sahimi, M.; Tsotsis, T. T. Removal of Trace Levels of Arsenic and Selenium from Aqueous Solutions by Calcined and Uncalcined Layered Double Hydroxides (LDH). *Ind. Eng. Chem. Res.* **2005**, *44*, 6804–6815.

(15) Prasanna, S. V.; Kamath, P. V. Chromate Uptake Characteristics of the Pristine Layered Double Hydroxides of Mg with Al. *Solid State Sci.* **2008**, *10*, 260–266.

(16) El Gaini, L.; Lakraimi, M.; Sebbar, E.; Meghea, A.; Bakasse, M. Removal of Indigo Carmine Dye from Water to Mg—Al—CO_3—calcined Layered Double Hydroxides. *J. Hazard. Mater.* **2009**, *161*, 627–632.

(17) Géraud, E.; Bouhent, M.; Derriche, Z.; Leroux, F.; Prévot, V.; Forano, C. Texture Effect of Layered Double Hydroxides on Chemisorption of Orange II. *J. Phys. Chem. Solids* **2007**, *68*, 818–823.

(18) Auxilio, A. R.; Andrews, P. C.; Junk, P. C.; Spiccia, L. The Adsorption Behavior of C.I. Acid Blue 9 onto Calcined Mg—Al Layered Double Hydroxides. *Dyes Pigm.* **2009**, *81*, 103–112.

(19) Auxilio, A. R.; Andrews, P. C.; Junk, P. C.; Spiccia, L.; Neumann, D.; Raverty, W.; Vanderhoek, N. Adsorption and Intercalation of Acid Blue 9 on Mg—Al Layered Double Hydroxides of Variable Metal Composition. *Polyhedron* **2007**, *26*, 3479–3490.

(20) Terry, P. A. Characterization of Cr Ion Exchange with Hydrotalcite. *Chemosphere* **2004**, *57*, 541–546.

(21) Ni, Z. M.; Xia, S. J.; Wang, L. G.; Xing, F. F.; Pan, G. X. Treatment of Methyl Orange by Calcined Layered Double Hydroxides in Aqueous Solution: Adsorption Property and Kinetic Studies. *J. Colloid Interface Sci.* **2007**, *316*, 284–291.

(22) Liu, Z.; Ma, R.; Osada, M.; Iyi, N.; Ebina, Y.; Takada, K.; Sasaki, T. Synthesis, Anion Exchange, and Delamination of Co—Al Layered Double Hydroxide: Assembly of the Exfoliated Nanosheet/Polyanion Composite Films and Magneto-optical Studies. *J. Am. Ceram. Soc.* **2006**, *128*, 4872–4880.

(23) Lee, J. H.; Rhee, S. W.; Jung, D. Y. Solvothermal Ion Exchange of Aliphatic Dicarboxylates Into the Gallery Space of Layered Double Hydroxides Immobilized on Si Substrates. *Chem. Mater.* **2004**, *16*, 3774–3779.

(24) Chen, H.; Zhang, F.; Fu, S.; Duan, X. In Situ Microstructure Control of Oriented Layered Double Hydroxide Monolayer Films with Curved Hexagonal Crystals as Superhydrophobic Materials. *Adv. Mater.* **2006**, *18*, 3089–3093.

(25) Besra, L.; Liu, M. L. A Review on Fundamentals and Applications of Electrophoretic Deposition (EPD). *Prog. Mater. Sci.* **2007**, *52*, 1–61.

(26) Sarkar, P.; Nicholson, P. S. Electrophoretic Deposition (EPD): Mechanism, Kinetics and Application to Ceramics. *J. Am. Ceram. Soc.* **1996**, *79*, 1987–2002.

(27) Shan, W.; Zhang, Y.; Yang, W.; Ke, C.; Gao, Z.; Ke, Y. Electrophoretic Deposition of Nano-size Zeolites in Non-aqueous Medium and Its Application in Fabricating Thin Zeolite Membranes. *Microporous Mesoporous Mater.* **2004**, *69*, 35–42.

(28) Sarka, P.; Mathur, S.; Nicholson, P. S.; Stager, C. V. Fabrication of Textured Bi—Sr—Ca—Cu—O Thick Film by Electrophoretic Deposition. *J. Appl. Phys.* **1991**, *69*, 1775–1777.

(29) Dougami, N.; Takada, T. Modification of Metal Oxide Semiconductor Gas Sensor by Electrophoretic Deposition. *Sens. Actuators, B* **2003**, *93*, 316–320.

(30) Du, C.; Heldbrant, D.; Pan, N. Preparation and Preliminary Property Study of Carbon Nanotubes Films by Electrophoretic Deposition. *Mater. Lett.* **2002**, *57*, 434–438.

(31) Oh, J. M.; Hwang, S. H.; Choy, J. H. The Effect of Synthetic Conditions on Tailoring the Size of Hydrotalcite Particles. *Solid State Ionics* **2002**, *151*, 285–291.

(32) Choy, J. H.; Jung, E. Y.; Son, Y. H.; Park, M. The Orientation of Anionic β- cyclodextrin in the Interlayer Space of Zn/Al Layered Double Hydroxide. *J. Phys. Chem. Solids* **2004**, *65*, 509–512.

(33) Gursky, J.; Blough, S.; Luna, C.; Gomez, C.; Luevano, A.; Gardner, E. Particle-particle Interactions Between Layered Double Hydroxide Nanoparticles. *J. Am. Ceram. Soc.* **2006**, *128*, 8376–8377.

(34) Beving, D. E.; Neill, C. R.; Yan, Y. S. Hydrophilic and Antimicrobial Low-silica-zeolite LTA and Hgh-silica-zeolite MFI Hybrid Coatings on Aluminum Alloys. *Microporous Mesoporous Mater.* **2008**, *108*, 77–85.

(35) Ho, Y. S.; Mackay, G. Pseudo-second Order Model for Sorption Processes. *Process. Biochem.* **1999**, *34*, 451–465.

(36) Azizian, S. Kinetic Models of Sorption: a Theoretical Analysis. *J. Colloid Interface Sci.* **2004**, *276*, 47–52.

(37) Safa Özcan, A.; Özcan, A. Adsorption of Acid Dyes from Aqueous Solutions onto Acid-activated Bentonite. *J. Colloid Interface Sci.* **2004**, *276*, 39–46.

(38) Goh, K. H.; Lim, T. T.; Dong, Z. L. Application of Layered Double Hydroxides for Removal of Oxyanions: A Review. *Water Res.* **2008**, *42*, 1343–1368.

(39) Xu, Z. P.; Stevenson, G.; Lu, C. Q.; Lu, G. Q (Max). Dispersion and Size Control of Layered Double Hydroxide Nanoparticles in Aqueous Solutions. *J. Phys. Chem. B* **2006**, *110*, 16923–16929.